AGU PUBLICATIONS

Water Resources Research

RESEARCH ARTICLE
10.1002/2015WR018250

Special Section:
Disturbance Hydrology

Extraordinary sediment delivery and rapid geomorphic response following the 2008–2009 eruption of Chaitén Volcano, Chile

Jon J. Major[1], Daniel Bertin[2], Thomas C. Pierson[1], Álvaro Amigo[2,3], Andrés Iroumé[4], Héctor Ulloa[4], and Jonathan Castro[5]

[1]U.S. Geological Survey, Volcano Science Center, Cascades Volcano Observatory, Vancouver, Washington, USA, [2]Servicio Nacional de Geología y Minería, Temuco, Chile, [3]Centro de Excelencia en Geotermia de los Andes, Universidad de Chile, Santiago, Chile, [4]Faculty of Forest Sciences and Natural Resources, Universidad Austral de Chile, Valdivia, Chile, [5]Institute of Geosciences, University of Mainz (Johannes Gutenberg Universität), Mainz, Germany

Key Points:
- Basins at Chaitén volcano released one of the greatest sediment yields following volcanic eruption
- Mean traction-load transport rates were very high, as great as several tens of kg s^{-1} m^{-1}
- Despite very high sediment delivery disturbed channels recovered rapidly

Supporting Information:
- Supporting Information S1
- Table S1
- Data Set S1
- Data Set S2
- Data Set S3

Correspondence to:
J. J. Major,
jjmajor@usgs.gov

Citation:
Major, J. J., D. Bertin, T. C. Pierson, Á. Amigo, A. Iroumé, H. Ulloa, and J. Castro (2016), Extraordinary sediment delivery and rapid geomorphic response following the 2008–2009 eruption of Chaitén Volcano, Chile, *Water Resour. Res.*, *52*, 5075–5094, doi:10.1002/2015WR018250.

Received 16 OCT 2015
Accepted 31 MAY 2016
Accepted article online 6 JUN 2016
Published online 2 JUL 2016

Abstract The 10 day explosive phase of the 2008–2009 eruption of Chaitén volcano, Chile, draped adjacent watersheds with a few cm to >1 m of tephra. Subsequent lava-dome collapses generated pyroclastic flows that delivered additional sediment. During the waning phase of explosive activity, modest rainfall triggered an extraordinary sediment flush which swiftly aggraded multiple channels by many meters. Ten kilometer from the volcano, Chaitén River channel aggraded 7 m and the river avulsed through a coastal town. That aggradation and delta growth below the abandoned and avulsed channels allow estimates of postdisturbance traction-load transport rate. On the basis of preeruption bathymetry and remotely sensed measurements of delta-surface growth, we derived a time series of delta volume. The initial flush from 11 to 14 May 2008 deposited 0.5–1.5 $\times$ 10^6 m^3 of sediment at the mouth of Chaitén River. By 26 May, after channel avulsion, a second delta amassed about 2 $\times$ 10^6 m^3 of sediment; by late 2011 it amassed about 11 $\times$ 10^6 m^3. Accumulated sediment consists of low-density vesicular pumice and lithic rhyolite sand. Rates of channel aggradation and delta growth, channel width, and an assumed deposit bulk density of 1100–1500 kg m^{-3} indicate mean traction-load transport rate just before and shortly after avulsion (~14–15 May) was very high, possibly as great as several tens of kg s^{-1} m^{-1}. From October 2008 to December 2011, mean traction-load transport rate declined from about 7 to 0.4 kg m^{-1} m^{-1}. Despite extraordinary sediment delivery, disturbed channels recovered rapidly (a few years).

1. Introduction

Explosive volcanic eruptions can drastically alter hydrogeomorphic regimes of drainage basins because volcanic processes can (1) severely damage vegetation, which decreases (or eliminates) foliar interception and reduces evapotranspiration [*Ayris and Delmelle*, 2012; *Swanson et al.*, 2013; *Pierson and Major*, 2014; *Crisafulli et al.*, 2015]; (2) deposit fine-grained tephra across broad swaths of landscape, which reduces surface infiltration and enhances overland flow [*Leavesley et al.*, 1989; *Yamakoshi et al.*, 2005; *Ogawa et al.*, 2007]; and (3) deposit extensive amounts of sediment along river channels, which alters channel hydraulics and can even reconfigure drainage networks [*Janda et al.*, 1984; *Punongbayan et al.*, 1996; *White et al.*, 1997; *Major and Mark*, 2006]. Hence, hydrogeomorphic responses in volcanically disrupted drainage basins can occur rapidly, produce greater-than-normal flows (and floods) for a given rainfall, trigger great releases of sediment, and sometimes persist for decades. Commonly, volcanically disturbed basins discharge short-term (several years) sediment yields (metric tons per square kilometer, t km^{-2}) that rival the world's greatest sediment-charged rivers [*Pierson and Major*, 2014].

The hydrogeomorphic response to the 2008–2009 eruption of Chaitén volcano, Chile, highlights the degree to which runoff regimes can be altered and the very high rates and magnitudes of sediment delivery that can follow volcanic disturbance. The eruption extensively, but variously, disturbed drainage basins proximal to the volcano. Tephra falls (volcanic "ash" falls) and pyroclastic density currents (PDCs) damaged dense rainforest vegetation in basin headwaters, draped hillsides with varying thicknesses and gradations of sediment, and deposited thick volcaniclastic fill in some valleys [*Carn et al.*, 2009; *Alfano et al.*, 2011; *Major and Lara*, 2013; *Major et al.*, 2013; *Pierson et al.*, 2013; *Swanson et al.*, 2013; *Umazano et al.*, 2014; *Ulloa et al.*, 2016]. South to southeast of the volcano, the eruption draped Chaitén and Negro River basins (Figure 1)

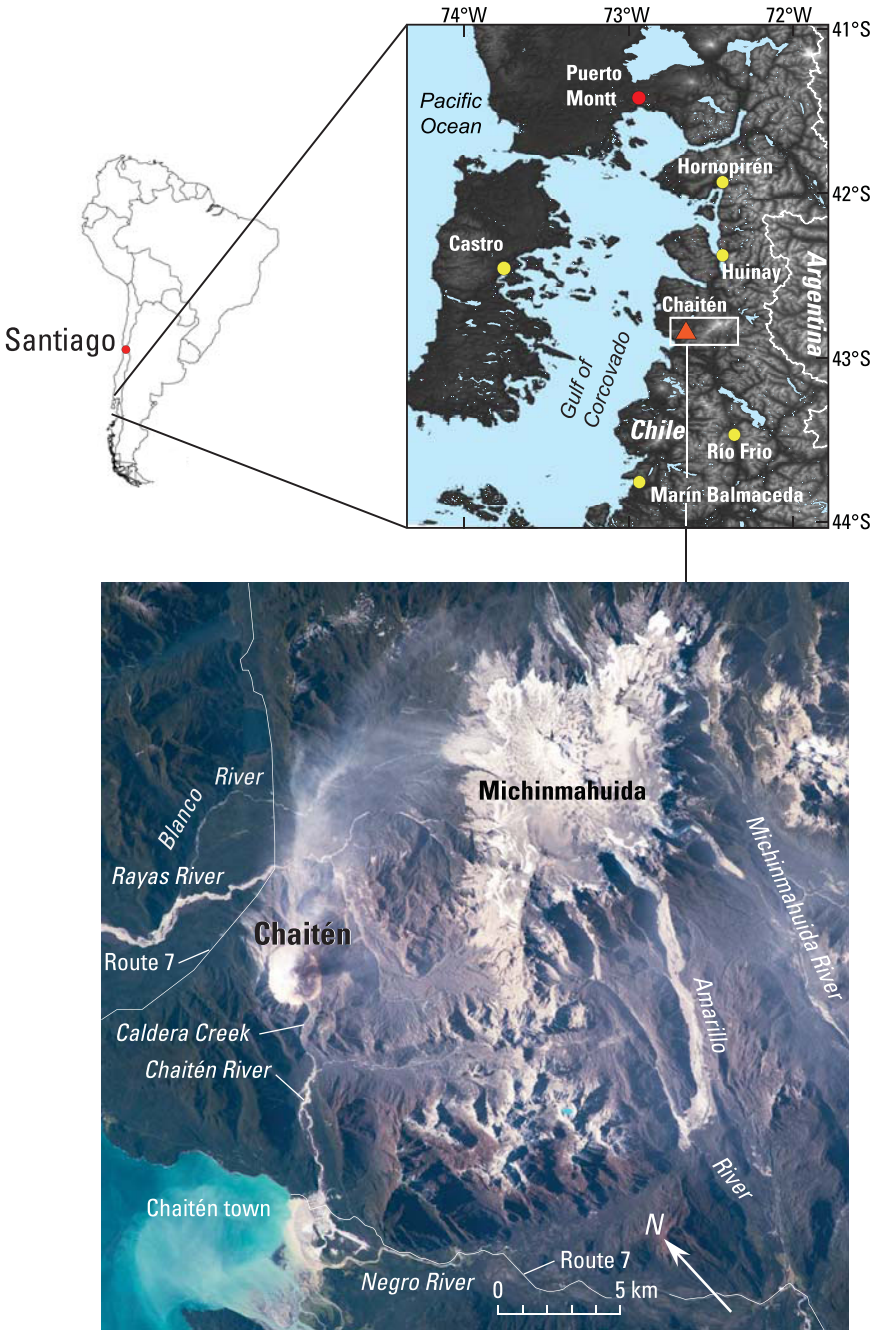

Figure 1. Location map of Chaitén volcano and named geographic features. Satellite image is International Space Station image ISS018-E-035716, taken 24 February 2009. Yellow dots in upper panel are sites of regional rain gages.

with tephra-fall deposits as thick as 200 cm; it also heavily damaged vegetation in Chaitén River basin headwaters, and PDC deposits twice filled the middle reach of Chaitén River channel. By contrast, vegetation in Negro River basin was not heavily damaged nor was its channel affected by PDCs.

Pierson et al. [2013] showed modest rainfall, which shortly followed the major phase of explosive activity, triggered an extraordinary sediment flush in the Chaitén River valley. Examination of stratigraphy, sediment texture, and photographs showed this sediment flush a complex, multiday event comprised of hyperconcentrated-flow lahar and muddy flood. Sediment mobilized by that lahar-flood event filled the lower 5 km of Chaitén River channel, buried the town of Chaitén (Figure 1) up to 3 m deep, and ultimately avulsed the river through town. Subsequent sediment delivery enlarged a delta in Chaitén Bay.

Here we quantify sediment delivery from Chaitén River basin, in terms of magnitude and rate, over a nearly 4 year period following onset of the eruption, and show it to be one of the greatest modern sediment releases following volcanic disturbance. We also show subsequent recovery to approximately preeruption channel condition was rapid. For logistical reasons, we focus on responses of Chaitén River basin, but show rapid and similar initial hydrogeomorphic responses were coeval in the Chaitén and Negro River basins. Though only limited sediment delivery estimates are calculable for Negro River basin, they lend perspective to the Chaitén River response.

This paper briefly summarizes the physiographic and climatic setting of Chaitén volcano, provides a synopsis of the eruption and its impacts on drainage basins, and discusses hydrogeomorphic response to those impacts. It compares the response at Chaitén to those of other volcanically disturbed fluvial systems, and discusses factors that influenced the response.

2. Physiographic and Climatic Settings

2.1. Physiography

Chaitén volcano (42.84°S, 72.65°W) is located in rugged topography of the Andean southern volcanic zone, about 10 km inland from the Pacific coast in northern Chilean Patagonia (Figure 1). Before its eruption the volcano consisted of a ~350 m high, 2 km diameter, rhyolite dome contained within a 3 km diameter caldera. The caldera's moat sat about 550 m asl and its rim altitude varied from about 700 to 900 m. Ridge crests of surrounding glaciated drainage basins range in altitude from about 800 to 1500 m.

The high-relief Chaitén, Negro, and Rayas River basins (Figure 1) drain proximal terrain in a broad sector east (and downwind) of the volcano, extending from the southwest around to the north and out to a distance of about 10 km. The rivers flow through glacially incised valleys having steep hillsides (50–70°) and broad floors that extend hundreds of meters from the active channels [*Ulloa et al*., 2015a, 2015b]. Channel gradients are steep and characteristic of mountain rivers: gradients of main stem channels over multikilometer reaches range from 0.0007 to >0.03, and steep tributary channels have gradients >0.23 (Table 1). Basin drainage areas range from 77 to 156 km^2 (Table 1). Other characteristics, such as active channel width (a few tens of meters), sinuosity index (slightly >1), and braiding index (~1) are provided by *Ulloa et al*. [2015a, 2015b]. Igneous and metamorphic bedrock in these watersheds is overlain by thin, highly permeable organic soils, generally <2 m thick. Prior to the eruption, dense temperate rainforest vegetation covered hillsides and valley floors, except

Table 1. Characteristics of Chaitén River and Negro River Channels and Drainage Basins

Drainage Basin Characteristic	Chaitén River	Negro River
Total basin area (km^2)	77	156
Percent of basin area having slopes >5%	93	78
Maximum basin relief, H (m)	1550	1550
Basin length, L_B (km)	16.8	13.5
Relief ratio, H/L_B	0.09	0.11
Average channel gradient		
Chaitén River		
Caldera Ck	0.236	
5 km—above Caldera Ck confluence	0.033	
7 km—below Caldera Ck confluence to bridge	0.016	
bridge to coast: original channel (2.8 km)	0.004	
avulsed channel (1.1 km)	0.009	
Negro River		
mountain tributary		0.082
5 km—valley floor above tributary confluence		0.003
4 km—valley floor tributary confluence to bridge		0.001
7 km—bridge to coast		0.0007
Approximate distance of basin centroid to Pacific coast along SW-NE line (km)[a]	9 (1)	18 (2)
Approximate distance of basin centroid to Chaitén volcano (km)	6	16
Azimuth of basin centroid from Chaitén volcano	South	South–southeast

[a]Number in parentheses represents number of intervening ridges ≥1000 m altitude between basin and Pacific Ocean.

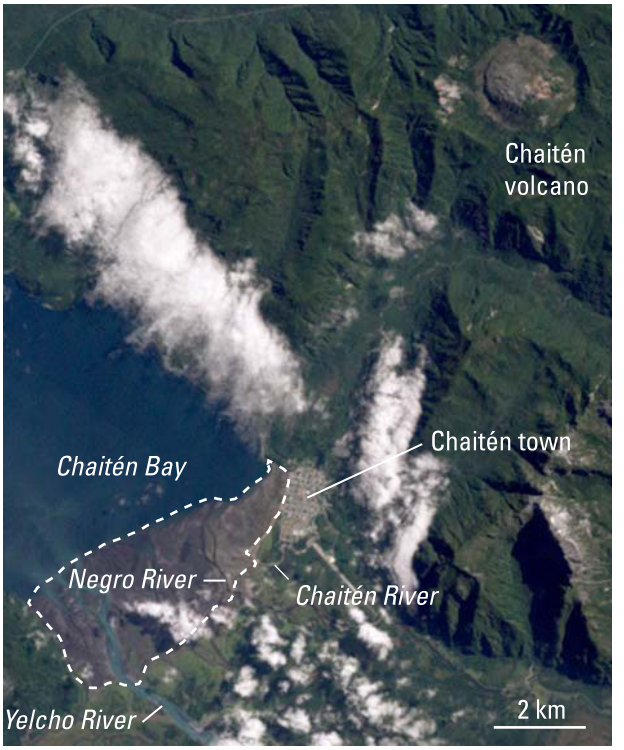

Figure 2. Preeruption Landsat image showing delta plain fed by sediment from Chaitén, Negro, and Yelcho rivers. Image chaitén_etm_2000052_landsat taken 21 February 2000.

in small scattered landslide scars and on active floodplains [*Major and Lara*, 2013; *Swanson et al.*, 2013; *Ulloa et al.*, 2015a, 2015b, 2016]. One tributary of Chaitén River, informally named Caldera Creek, drains the caldera through a breach in the south rim (Figure 1).

The region around Chaitén volcano is sparsely populated. The port town of Chaitén (preeruption population ~4000) lies at the mouth of Chaitén River valley along Chaitén Bay, 10 km downstream from the volcano (Figure 1). No major towns exist in the other river basins. The principal regional road (Route 7) passes along the northern base of the volcano, and to the south passes through Chaitén town and along the distal Negro River valley. A major ferry dock, serving the regional nautical transportation system, lies at the northwest edge of Chaitén town.

Prior to the eruption, a ~14 km^2 delta plain had formed in Chaitén Bay owing to sediment delivery by Chaitén, Negro, and Yelcho Rivers (Figure 2). It assumed a roughly SW–NE triangular shape, widest near the mouth of Yelcho River and tapering northeastward. Immediately west of town, the delta plain measured 800 m wide normal to its front before plunging steeply (gradient ~0.125) into the bay [*Servicio Hidrográfico y Oceanográfico de la Armada de Chile*, 1999]. The delta plain lay within the intertidal zone. Post-eruption sediment delivered by Chaitén River accumulated largely across the northeastern ~2.5 km^2 of the plain and along the plunging delta front.

2.2. Climate and Rainfall

Northern Patagonia (40°S–48°S latitude) receives abundant rainfall mainly from strong, moisture-laden frontal systems moving eastward from the southern Pacific Ocean [*Garreaud*, 2009]. Winter storms typically are spaced only a few days apart. Rainfall can occur nearly continuously for a month or more, and accumulations from individual storms (periods of continuous rainfall separated by at least 2 days of less than 5 mm of total rain) can be hundreds of mm [*Dirección General de Aguas*, 2015]. Annual precipitation in Chaitén town in the decade before the eruption ranged from 2600 to 4300 mm; in the broader region around the volcano, it ranged from about 1400 to 6600 mm [*Dirección General de Aguas*, 2015; *Fundación Huinay*, 2015]. River discharges are typically greatest May through August, but substantial discharge can persist through December before declining through austral summer.

3. Volcanic Disturbances to Drainage Basins

A variety of volcanic processes can damage vegetation, deposit sediment, and affect hydrogeomorphic balances of drainage basins [*Pierson and Major*, 2014]. Explosive eruptions commonly disturb landscapes through some combination of fall and flow processes. Principal disturbance agents during eruption of Chaitén were downwind tephra falls from eruption plumes [*Alfano et al.*, 2011] and PDCs caused by directed explosions, collapses of eruption plumes, and collapses of parts of an effusing lava dome [*Major and Lara*, 2013; *Major et al.*, 2013; *Swanson et al.*, 2013]. These volcanic processes severely disturbed the landscape and drastically altered the fluxes of water and sediment in proximal drainage basins.

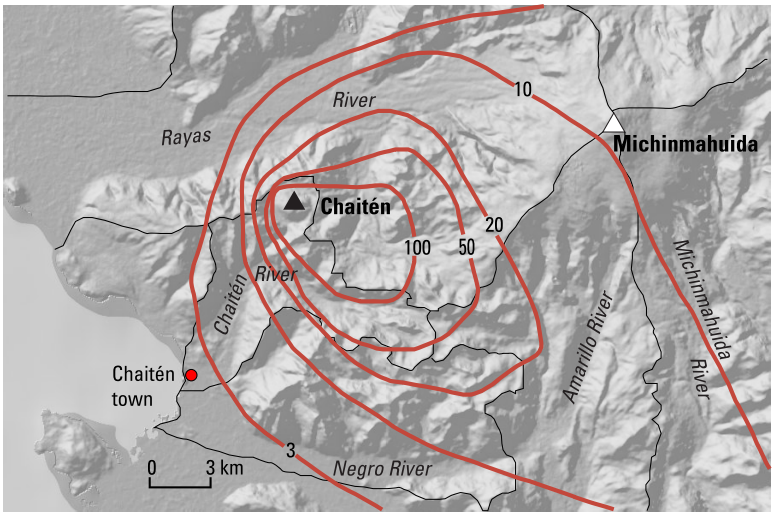

Figure 3. Isopach map of tephra fall around Chaitén volcano (in cm). Refined contours based on measurements of tephra thicknesses in headwater basins conform to more distal contours of *Alfano et al.* [2011]. Watershed boundaries delineated.

3.1. Synopsis of the 2008–2009 Eruption

Following centuries of dormancy [*Lara et al.*, 2013; *Watt et al.*, 2013; *Moreno et al.*, 2015], Chaitén volcano began erupting late in the evening of 1 May 2008 (local time, UTC-4) [*Carn et al.*, 2009; *Lara*, 2009; *Castro and Dingwell*, 2009; *Major and Lara*, 2013]. The eruption consisted of an explosive phase (1–11 May), a transitional phase involving explosions and concurrent lava extrusion (~12–31 May), and a prolonged effusive phase (June 2008 to December 2009) in which a large lava dome extruded [*Pallister et al.*, 2013].

The explosive initial phase of the eruption (Volcanic Explosivity Index value 4–5) [see *Newhall and Self*, 1982] produced intermittent large explosions from 2 to 8 May. This phase of eruption dispersed tephra falls generally eastward [*Carn et al.*, 2009; *Watt et al.*, 2009; *Alfano et al.*, 2011; *Prata et al.*, 2015], but the sequence of eruption plumes deposited a complex succession of tephra-fall layers from N to SW in basins proximal to the volcano. Partial collapses of the newly emplaced lava dome [*Pallister et al.*, 2013] produced two lithic-rich PDCs—one in mid to late 2008 and the other on 19 February 2009 [*Major et al.*, 2013]. These two PDCs deposited 8–10 m thick volcaniclastic fill in the middle reach of Chaitén River valley, below the confluence with Caldera Creek (Figure 1).

3.2. Tephra Fall

Tephra falls draped basin headwaters in a sector NE to S of the volcano (Figure 3) [*Alfano et al.*, 2011]. Deposits varied in thickness from 2 to over 100 cm, and locally exceeded 200 cm (Figure 3). However, isopachs are based largely on thickness measurements made beginning in January 2009 [*Alfano et al.*, 2011] following compaction and erosion of tephra by a few meters of posteruption rainfall. Heights of ash pedestals (sheltered from raindrop erosion and compaction by fallen leaves or branches) indicate as much as 10 cm of the ash blanket may have eroded or compacted locally before it was measured. Accumulations are greatest in headwaters of basins nearest the volcano—the Rayas and Chaitén basins—with mean thicknesses of 55 and 35 cm, respectively (Figure 3 and Table 2). The eruption draped the more southerly Negro basin, outside the principal plume trajectory, with an average tephra thickness of about 8 cm.

Table 2. Tephra Deposit Thicknesses and Volumes in the Drainage Basins Near Chaitén Volcano[a]

Tephra Fall Distribution	Chaitén River Basin	Negro River Basin	Rayas River Basin
Drainage basin area upstream of bridge (km^2)	73	127	114
Estimated minimum tephra thickness (cm)	3	2	2
Estimated maximum tephra thickness (cm)	200+	50	200+
Estimated mean tephra thickness (cm)	35	8	55
Estimated tephra volume (million m^3)	25	10	60

[a]Values are minima because significant erosion of tephra mantle occurred prior to thickness measurements at most sites.

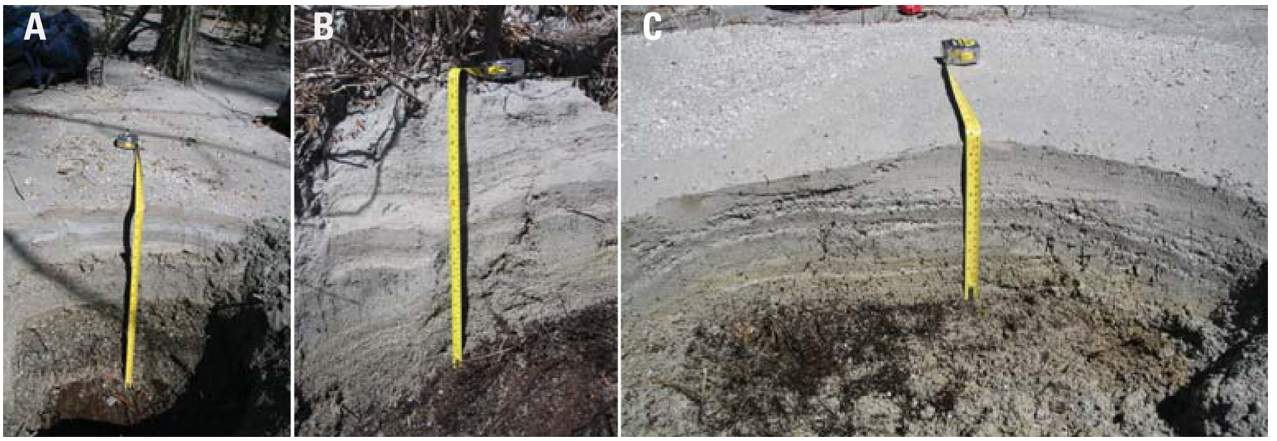

Figure 4. Sections of tephra-fall deposits from affected drainage basins, all showing fine-grained surface layers. (a) Rayas River basin near mouth of channel draining east side of Chaitén volcano (see Figure 1); coarse-grained lapilli layer, called β-layer [*Alfano et al*., 2011], is near section base. (b) East fork of Chaitén River channel about 5 km upstream of confluence with Caldera Creek (see Figure 1). (c) Headwaters of Negro River about 400 m from drainage divide with Chaitén River basin. USGS photos by R. P. Hoblitt, 22–24 January 2010.

The tephra-fall sequence within 10–15 km of the volcano generally fines upward from basal fine lapilli (about 2–4 mm) and coarse to medium ash (about 0.25–1 mm) to fine and very fine ash (0.25–0.063 mm) (Figure 4) [*Alfano et al*., 2011; *White and Houghton*, 2006, nomenclature]. In general, fine to very fine ash composes the upper 20% of the fall-deposit sequence in basin headwaters. Vigorous and sustained eruption plumes from 3 to 5 May deposited much of the fall deposits in the Chaitén River and Negro River basins [*Alfano et al*., 2011]. Additional vigorous explosions on 6 and 8 May also dispersed tephra across basin headwaters, and less vigorous ash emissions persisted throughout the waning phase of explosive activity [*Alfano et al*., 2011; *Major and Lara*, 2013].

The great amount of fine to very fine ash in the upper part of the tephra blanket possibly decreased hillside infiltration capacities by as much as 2 orders of magnitude compared to preeruption values [*Pierson and Major*, 2014]. In addition to its fine particle size, physical and chemical processes acting within the upper few mm of the ash also may have contributed to reduced infiltration capacity [*Pierson and Major*, 2014]. Such virtual sealing of hillsides to infiltration can increase direct runoff ratios to as much as 90% [*Yamakoshi et al*., 2005; *Pierson and Major*, 2014]. These hydrological modifications to the landscape, in addition to heavy vegetation damage caused by the eruption [*Swanson et al*., 2013], almost certainly increased the volume and rate of direct runoff in the volcanically disturbed basins.

Erupted products included lithic, obsidian, and pumice components. Erupted pumice, the major component of the tephra fall, had bulk densities ranging from 400 to 1300 kg m^{-3}, with a primary mode of 700 kg m^{-3} [*Alfano et al*., 2012]. Obsidian and lithic particles had higher densities. Densities of water-soaked fine pumice lapilli from Chaitén River deposits ranged from 1300 to 1600 kg m^{-3}.

3.3. Pyroclastic Density Currents

Dome collapses during the effusive phase of eruption triggered two PDCs that swept through the breach in the south caldera wall and funneled into the middle reach of Chaitén River valley [*Major et al*., 2013; *Pallister et al*., 2013]. The latter flow in February 2009 traveled about 7 km to within 3 km of Chaitén town, and deposited 3–5 $\times$ 10^6 m^3 of very poorly sorted, unstratified, lithic-rich gravelly sand as much as 8–10 m deep [*Major et al*., 2013]. The earlier 2008 deposit, of similar composition, had been largely reworked prior to the 2009 flow; thus, its original thickness and distribution are not known, but it did not extend beyond the distal limit of the 2009 deposit.

4. Methods

Analysis of sediment delivery following eruptive disturbance relied on field investigations of deposit character and stratigraphy, limited surveys of channel geometries, analysis of satellite images and aerial photographs, and estimates of the relative proportions of suspended and traction-load sediment. The basins lacked gage measurements of water or sediment flux; hence, estimates of sediment flux—and the nature of

transport events—are reconstructed from rates and magnitudes of channel fill and delta growth, and character of deposits. Owing to remote and rugged terrain and dense vegetation, ground investigations were restricted to areas accessible near roads and to medial to distal channel reaches. In 2010, we had limited helicopter support to examine deposits in basin headwaters.

4.1. Tephra Volume Calculations

New measurements of tephra thickness in basin headwaters together with previously published isopach maps at more distal sites provide estimates of tephra volumes in proximal watersheds. Estimated tephra thicknesses in 1 km^2 (UTM grid) cells were interpolated linearly on 1:50,000 maps having isopachs adjusted to reflect additional basin headwater data but constructed to conform with those from a previous study [*Alfano et al*., 2011]. Tephra thicknesses (and volumes) within each cell in each drainage basin were summed to estimate total tephra volumes per basin (Table 2). Linear interpolation between isopachs likely underestimates local tephra thickness within 5–10 km by several cm and overestimates thickness beyond because thickness commonly decreases exponentially over tens to hundreds of km distance from source [*Bonadonna and Costa*, 2013]. However, the greatest error in estimates of tephra volume in each basin results not from linear interpolation between isopachs ($\leq$3 km), but from isopachs being based on limited thickness measurements taken after tephra had been eroded. In proximal basins, we therefore consider reported tephra volumes to be minimum values.

4.2. Interpretation of Satellite Images and Aerial Photographs

Chaitén River originally flowed past Chaitén town and emptied into Chaitén Bay 13.5 km downstream of the caldera center (Figures 1 and 2). Posteruption sediment delivery induced rapid accumulation of new deltaic deposit atop the older delta plain. Initially, new deltaic sediment (delta 1) deposited at the mouth of Chaitén River near the mouth of Negro River. However, infilling of the distal 3.5 km of channel during an initial phase of rapid aggradation [*Pierson et al*., 2013] avulsed the river through town beginning about 14–15 May. That avulsion induced sediment accumulation in a second delta (delta 2) just north of the original river mouth (Figures 5 and Supporting Information Figures S1–S3).

We used a variety of images to estimate timing, extent, and rate of channel sedimentation, and extents and rates of delta growth. Oblique aerial photographs from low-altitude helicopter overflights during the eruption provided constraints on the initial timing, extent, and rate of channel sedimentation in lower Chaitén River. Objects of known dimension (fence posts, bridge piers, bridge railings, etc.) provided scale to quantify channel aggradation. We assume aggradation estimates have errors of about $\pm$0.5 m. Initial Chaitén River results are reported in *Pierson et al*. [2013]. We measured visible delta growth in Chaitén Bay on rectified images from various remote sensing platforms (ASTER, Advanced Land Imager (ALI), Landsat, International Space Station (ISS), Formosat, and DigitalGlobe; Figures S1–S3 and Text S1 in Supporting Information). Areas measured independently were mostly within 0.1–0.15 km^2.

Magnitudes and rates of delta growth from 2008 to 2012 provided estimates of mean traction-load transport rates by Chaitén River. Preavulsion deltaic sediment covered an area of 0.55 ± 0.1 km^2 and had an assumed average deposit thickness of about 2 m [*Pierson et al*., 2013]. Postavulsion deltaic sediment filled both the preeruption intertidal and the posteruption supratidal zones. Temporal changes of delta volume were estimated by measuring areas of the growing delta (error 0.1–0.15 km^2) visible in satellite images, normalizing them to a zero-tide-height sea level, and multiplying those normalized areas by an estimated thickness of the deltaic sediment (Text S1 and Data Set S1 in the Supporting Information). Some traction load likely bypassed the supratidal and intertidal accumulation zones and deposited along the steep delta front, but we have little data to confidently constrain that volume. We assume estimated delta volumes over time, exclusive of sediment accumulated along the delta front, have errors of 10–15%.

Relations between traction load and total sediment load are used to estimate total sediment delivery, because suspended-sediment concentration was not measured (except sporadically at low flow). If we assume traction load composed 20–50% of the total sediment load—a range common in mountain rivers, even in those that experience very high sediment loading [e.g., *Hammond*, 1989; *Wohl*, 2000; *Pelpola and Hickin*, 2004; *Pratt-Sitaula et al*., 2007; *Turowski et al*., 2010; *Major et al*., 2012; *Magirl et al*., 2015]—then we can broadly estimate possible annual sediment loads delivered from the basin for the first few years after onset of eruption.

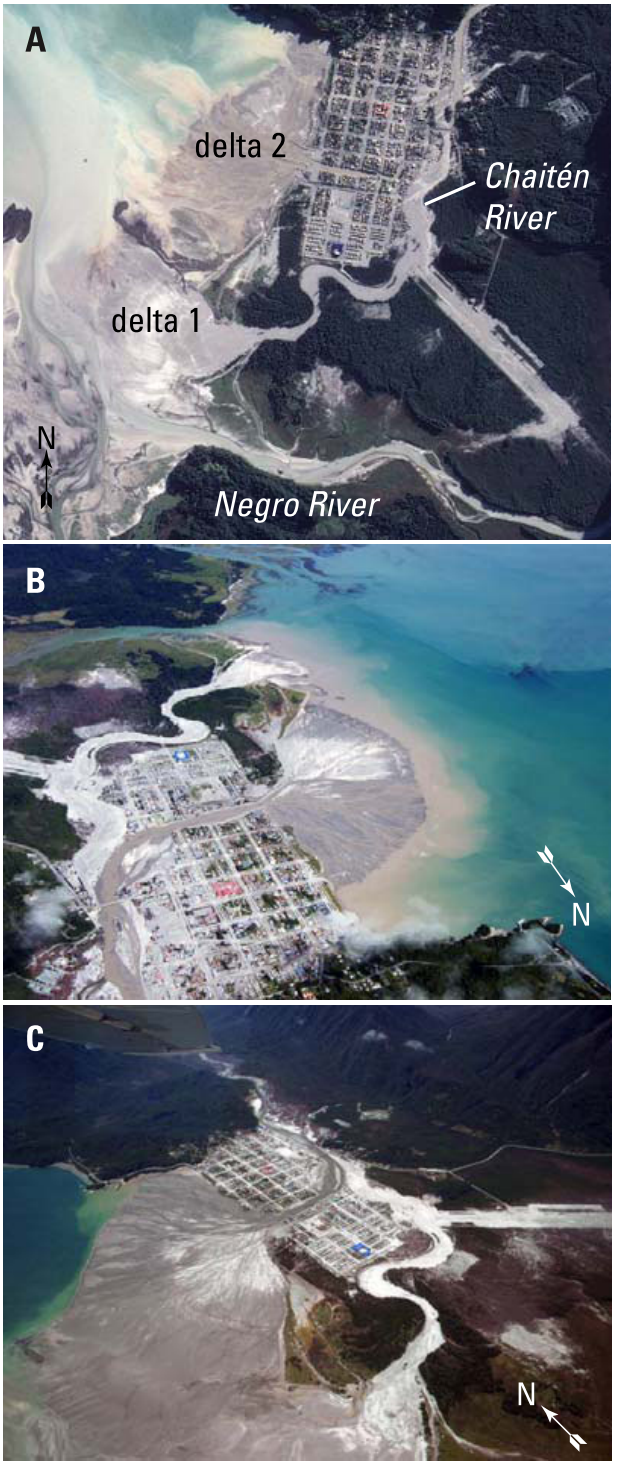

Figure 5. Images of delta growth at mouth of Chaitén River. (a) Formosat image 2008147, taken 26 May 2008. (b) Oblique aerial view looking downstream. Photograph by P. Duhart, SERNAGEOMIN, February 2009. (c) Oblique aerial view looking upstream. Photograph by E. Manríquez, December 2010.

4.3. Rainfall

Rainfall to drainage basins around Chaitén volcano was estimated by proxy [*Pierson et al.*, 2013]. It could not be measured directly, because rainfall data are available only from widely dispersed rain gages in northern Patagonia (Figure 1). The gage closest to Chaitén is at Huinay (~60 km NNE; Figure 1), situated on the shore of a narrow fjord oriented NNW and sandwiched between steep ridges rising to about 1000 m. This gage is assumed to record orographic rainfall representative of the upper Chaitén and Negro River basins, which are at similar distances inland and have watershed divides at similar altitudes. The Río Frio gage (~78 km SSE; Figure 1) is located in a north-south inter-Andean valley 60 km inland from the coast and in the rain shadow of a ridge 1200–1500 m in altitude. Prior to the eruption, a rain gage existed near the mouth of Chaitén River, but it was destroyed by tephra fall. For several years prior to 2008, that rain gage and the one at Río Frio collected very similar rainfall amounts [*Dirección General de Aguas*, 2015]. We assume an average of the measurements at Huinay and Río Frio is roughly representative of overall rainfall in the Chaitén and Negro River basins [*Pierson et al.*, 2013]. Estimates of rainfall amounts are not critical to our estimates of sediment volumes and transport rates, but they provide perspective on the hydrological modifications effected by the eruption and the postdisturbance sensitivity of the landscape to those hydrological changes.

5. Fluvial System Responses to Disturbance

5.1. Initial Sediment Delivery Following Volcanic Disturbance (May 2008)

Extraordinary sediment delivery from hillsides to channels defined the initial geomorphic response to volcanic disturbance in proximal drainage basins. Abundant erosion of the tephra mantle (Figure 6) by overland flow delivered great quantities of sediment to channels; thick deposits extend 4–7 m above preeruption channel beds along the Chaitén and Negro River channels. These sediments were transported initially by hyperconcentrated flow (perhaps as much as 15–30% sediment by volume [e.g., *Pierson*, 2005; *Wilcox et al.*, 2014]), followed gradually by

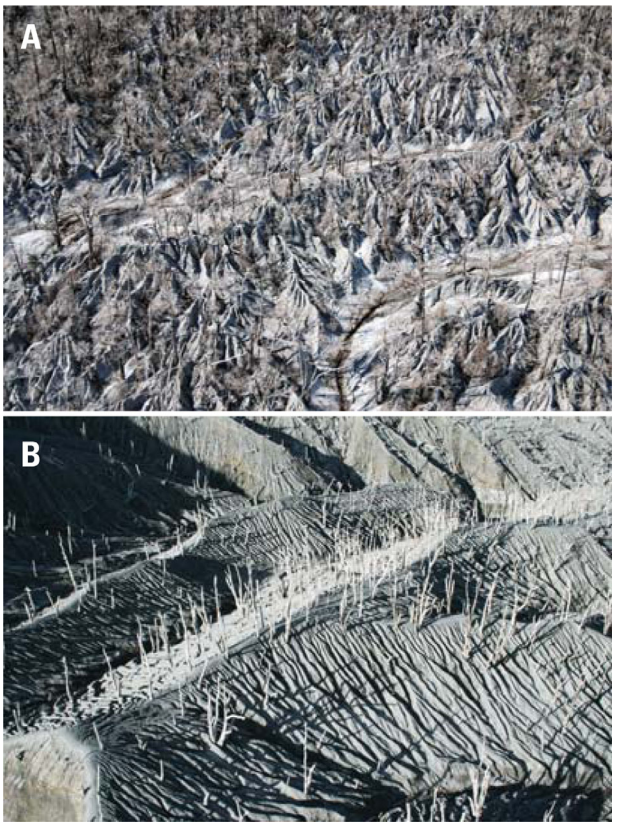

Figure 6. Photographs of tephra erosion near drainage divide between Chaitén River and Rayas River basins, about 2 km southeast of caldera. Both show trees stripped of branches, understory vegetation buried by roughly 2 m of tephra-fall deposit, and extensive rill and gully erosion. Photograph (a) by J. J. Major and (b) by T. C. Pierson, USGS, 21 January 2010.

sediment-laden flood flow [*Pierson et al.*, 2013]. Transport predominantly by dilute hyperconcentrated flow and fluvial processes at Chaitén contrasts with responses at many volcanoes worldwide, where syneruption and initial posteruption rainfalls commonly trigger debris flows and high-concentration hyperconcentrated flows from tephra-laden landscapes [*Waldron*, 1967; *Umbal*, 1997; *Miyabuchi*, 1999; *Lavigne et al.*, 2000; *Barclay et al.*, 2007; *Pierson and Major*, 2014; *Jones et al.*, 2015].

5.1.1. Chaitén River

Modest, low-intensity rainfall during the waning stages of explosive activity triggered abundant erosion of hillside tephra and extraordinary sediment delivery to the distal Chaitén River channel [*Pierson et al.*, 2013]. Light rainfall began on 11 May (~20 mm in 24 h; 30 min intensities $\leq$3 mm h^{-1}; Figures 7A and 7B), and within 72 h the lower 3.5 km of Chaitén River channel aggraded as much as 7 m, almost 5 m of which aggraded within the first 24 h [*Pierson et al.*, 2013]. The unusual nature of this event is highlighted by the simultaneously pedestrian discharges of several regional rivers (Figure S4 in Supporting Information). Sediment particles in the channel fill are composed dominantly of fresh, gray lithic rhyolite and gray to white poorly vesicular pumice sand, showing eroded new tephra [*Alfano et al.*, 2011] was the principal source of sediment, not older material eroded from channel storage.

On the basis of measurements from satellite images and aerial photographs, *Pierson et al.* [2013] estimated 3–8 $\times$ 10^6 m^3 of sediment deposited along the lower 7–9 km of the original channel and in a delta at its mouth over a span of 2–3 days. They estimated 2–5 $\times$ 10^6 m^3 of sediment filled the lower channel and 1–3 $\times$ 10^6 m^3 of sediment accumulated in the delta. Reanalysis of satellite images and aerial and field photographs indicates fill from the initial sediment flush accumulated over 0.5 km^2 within the lower 5 km channel reach and that it tapers upstream. Therefore, its average thickness is perhaps 4–5 m. Furthermore, sediment (~1–3 m thick) accumulated across about 0.55 km^2 of the preeruption delta plain (delta 1), rather than 0.85 km^2 estimated by *Pierson et al.* [2013]. This reanalysis indicates bed-material fill from the initial sediment flush was perhaps 2–3 $\times$ 10^6 m^3 rather than 2–5 $\times$ 10^6 m^3, and the initial delta accumulated about 0.5–1.5 $\times$ 10^6 m^3 of sediment rather than 1–3 $\times$ 10^6 m^3.

Analyses of deposit lithofacies indicate sediment deposited under conditions ranging from hyperconcentrated flow to very muddy streamflow [*Pierson et al.*, 2013; *Umazano et al.*, 2014]. Sedimentary structures and textures of channel fill range from massive to horizontally stratified, poorly sorted, pumice-rich medium sand containing fine gravel in the lower two thirds of the fill to cross-bedded, pumice-rich medium sand containing fine gravel in the upper third (Figures 8A and 8B). The structures and textures indicate high-concentration hyperconcentrated flow to perhaps dilute debris flow emplaced the lower 2 m of exposed fill (type A deposits [*Pierson et al.*, 2013]), and dilute hyperconcentrated flow and muddy streamflow under upper-flow-regime (supercritical turbulent flow) conditions emplaced the superjacent 2 m (type B deposits [*Pierson et al.*, 2013]). Traction load under shallow, braided channel conditions deposited the upper

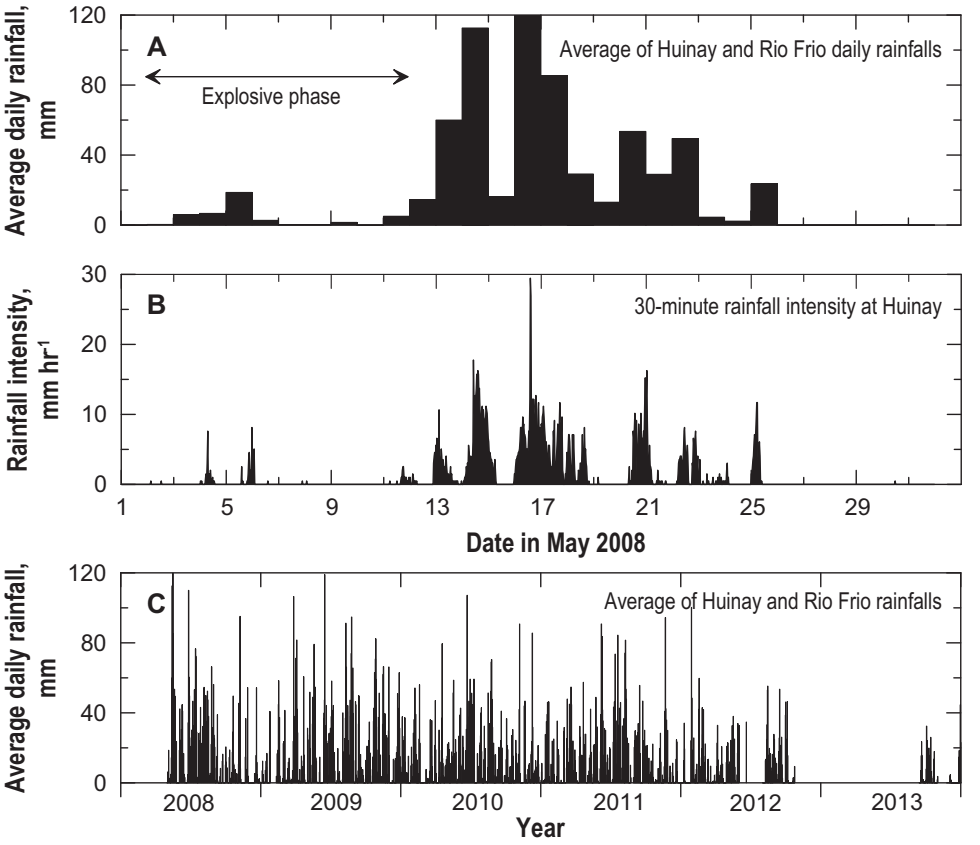

Figure 7. Rainfall in vicinity of Chaitén volcano. (a) Averaged daily rainfall from gages at Huinay and Río Frio (see Figure 1 for gage locations). (b) Rainfall intensities measured at Huinay. Panels from *Pierson et al.* [2013]. (c) Long-term averaged daily rainfall from gages at Huinay and Río Frio.

~1–1.5 m of fill (type C deposits [*Pierson et al.*, 2013; *Umazano et al.*, 2014]), though grain-size analyses indicate flow likely carried much suspended sediment [*Pierson et al.*, 2013].

Volumetric estimates of sediment delivery are based on sediment-transport process. Mass flow or flow transitional to fluvial flow deposited much of the initial channel and delta fill prior to avulsion. Volumetric estimates of sediment delivery by these processes are limited to estimated deposit volumes. However, the fluvial character of the upper 1–1.5 m of fill, deposited mainly by traction load, allows us to extend estimates of total sediment delivery by assuming traction load represents about 20–50% of the fluvially transported sediment. On the basis of channel fill and delta volumes above, and on assumptions about the percentage of fill associated with mass flow versus fluvial processes (~2/3 mass flow, 1/3 fluvial), hyperconcentrated flow delivered at least 1.5–3 $\times$ 10^6 m^3 of the initial sediment flush and fluvial transport delivered about 0.75–1.5 $\times$ 10^6 m^3 (Table 3). Because sediment texture and composition indicate streamflow carried much suspended sediment, some of the fluvially deposited fill may represent suspended sediment caught during traction-load deposition. *Visher* [1969] proposed grain-size distributions of fluvially deposited sediment consist of subpopulation distributions transported by different processes. He hypothesized distinct linear segments within the overall grain-size distribution when plotted in log-probability space can differentiate subpopulations resulting from suspended-load and traction-load deposition. On the basis of this hypothesis, grain-size analyses of samples of the fluvial channel fill indicate it may contain, on average, 20–30% suspended sediment caught during traction-load deposition (Figure S5 in Supporting Information). Hence, traction load may account for only 0.5–1 $\times$ 10^6 m^3 of the initial channel and delta fill.

Estimates of mass-flow and traction-load volumes permit an estimate of possible total sediment delivery by the preavulsion sediment flush. Using estimated traction-load volumes and assumptions about the ratio of traction load to total fluvial load, we estimate the volume of sediment transported fluvially during the initial sediment flush of 11–12 May was perhaps 1–5 $\times$ 10^6 m^3. Thus, minimum total delivery during that

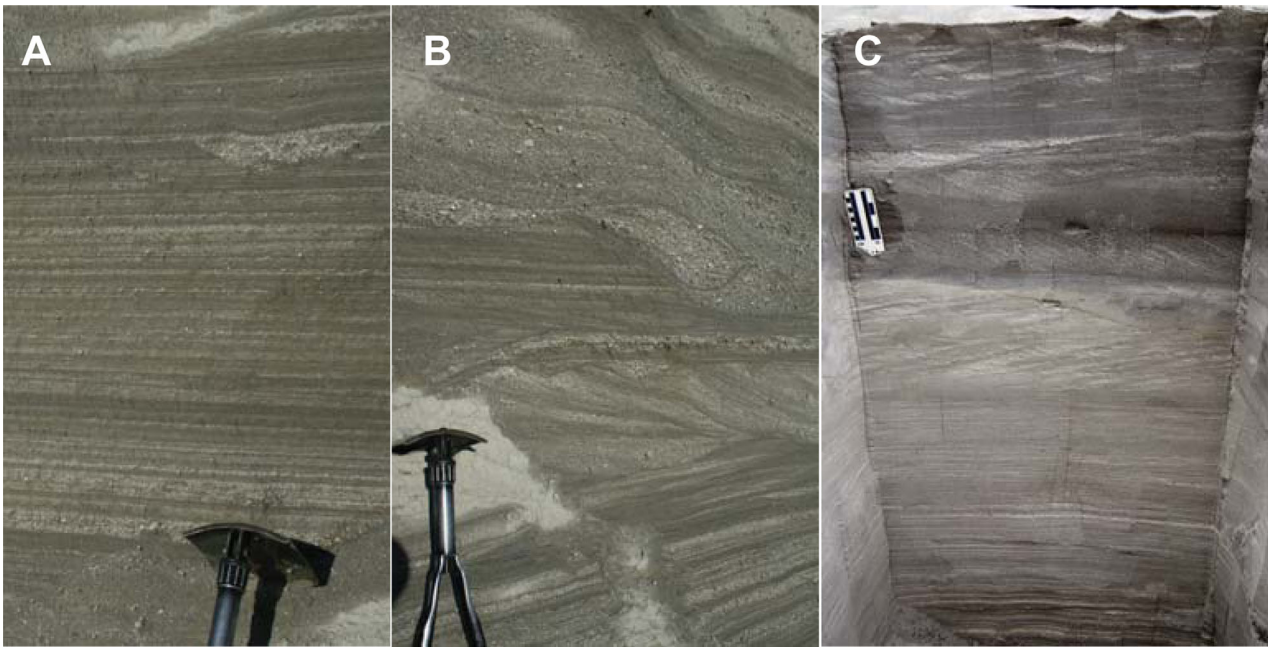

Figure 8. Lithofacies of deposits emplaced in Chaitén and Negro River channels about 3 and 7.3 km upstream of river mouths, respectively. (a) Horizontally bedded sand in lower part of Chaitén River deposit sequence shows thin beds and lenses of segregated pumice granules (type B deposits of *Pierson et al.* [2013]). Dilute hyperconcentrated flow or highly concentrated, muddy streamflow deposited this sediment. Shovel blade is 15 cm wide. (b) Stratified sediment having high-angle cross beds (type C deposits of *Pierson et al.* [2013]) alternating with zones of type B deposits. Dilute muddy streamflow during later stages of the flood event deposited type C lithofacies sediment. Figures 8a and 8b are from *Pierson et al.* [2013]. (c) Horizontally bedded sand in lower part of Negro River deposit sequence shows thin beds and lenses of segregated pumice granules. The horizontally bedded sand grades upward to ripple-drift cross-bedding. Dark-colored sand with dune-scale planar cross-bedding and lying above erosional contact is deposited on a bench cut into the main sequence. USGS photographs (a) and (b) by T. C. Pierson, (c) by J. J. Major.

sediment flush, including hyperconcentrated flow, was perhaps 3–8 $\times$ 10^6 m^3. If we further assume a bulk deposit density of 1100–1500 kg m^{-3} for the pumice-rich fluvial deposits and about 1750 kg m^{-3} for the hyperconcentrated flow deposit [e.g., *Wilcox et al.*, 2014], then these volumetric estimates indicate an initial sediment yield of perhaps 40–200 kt km^{-2} (Table 3). Tephra fall deposited a minimum 25 $\times$ 10^6 m^3 of ash (<2 mm) and minor lapilli (2–64 mm) across Chaitén River basin (Table 2) and perhaps as much as 30 $\times$ 10^6 m^3. Our estimates of initial sediment delivery indicate perhaps 10–30% of that tephra was eroded within days.

Rates of channel aggradation and delta growth owing to traction-load transport indicate mean traction-load transport rate (of sand) just before avulsion (11–14 May) was perhaps 20–80 kg s^{-1} m^{-1} (Table 3). Such a transport rate is very high but not unprecedented; measured rates in gravel bed rivers transporting great amounts of bed load have ranged from 2 to 20 kg s^{-1} m^{-1} [e.g., *Bagnold*, 1977; *Childers*, 1999; *Pitlick*, 1992; *Laronne and Reid*, 1993; *Reid et al.*, 1997; *Pitlick et al.*, 2009; *Wallick et al.*, 2010; *Major et al.*, 2012; *Magirl et al.*, 2015], but have been as great as 60 kg s^{-1} m^{-1} during desert flash floods [*Cohen and Laronne*, 2005]. Traction-load transport rates in sand-bed rivers typically are <0.01–1 kg s^{-1} m^{-1} [e.g., *Bagnold*, 1977; *Dietrich and Smith*, 1984; *Gaweesh and van Rijn*, 1994; *Rennie and Villard*, 2004; *Gaeuman and Jacobson*, 2006]. Measured bed load transport rates at low-flow (2–12 m^3 s^{-1}) in summers 2010–2015 in lower Chaitén River were 0.001–5.7 kg s^{-1} m^{-1} (A. Iroumé, Univ. Austral de Chile, unpublished data). For comparison, low-flow bed load transport rates in heavily impacted, braided rivers at Mount Pinatubo (Philippines) 6 years after its 1991 eruption were as great as 1.6 kg s^{-1} m^{-1} [*Montgomery et al.*, 1999; *Hayes et al.*, 2002]. At Chaitén, the waning stage of the initial sediment flush, when normalized by the 5 km length of channel aggraded, produced a streamwise-normalized mean transport rate of about 4–16 kg s^{-1} m^{-1} per km of channel. Unlike the very modest rainfall that triggered the initial 5 m of channel fill predominantly by hyperconcentrated flow, the waning stage fluvial flush happened during heavier rainfall (about 190 mm from 12 through 14 May; Figure 7A). Very high sediment delivery greatly altered channel character. The channel became significantly smoother and wider, and developed a shallow, braided channel pattern [*SERNAGEOMIN*, 2008b].

AGU Water Resources Research

10.1002/2015WR018250

Table 3. Estimates of Volumetric and Mass Sediment Delivery and Traction-Load Transport Rates From Chaitén River Basin

Date	Channel Fill Lahar Deposit Thickness (m)[a]	Channel Fill Fluvial Deposit Thickness (m)[a]	Channel and Delta 1 Lahar Volume (10^6 m^3)[b]	Channel and Delta 1 Fluvial Volume (10^6 m^3)[b]	Channel and Delta 1 Traction-Load Volume (10^6 m^3)	Delta 2 Volume (10^6 m^3)	Cumulative Traction-Load Volume (10^6 m^3)	Traction-Load Transport Rate (kg/s/m)[c]	Cumulative Fluvial Transport (10^6 m^3)		Cumulative Fluvial Sediment Delivery (10^6 m^3)	Cumulative Fluvial Mass Transport (10^6 t)[d]	Lahar Mass Transport (10^6 t)[e]	Cumulative Mass Delivery (10^6 t)	Cumulative Sediment Yield (10^6 t/km^2)[f]
									Bed Load (20%)	Bed Load (50%)					
2008															
15 May	4–6	1–1.5	1.5–3	0.75–1.5	0.5–1		0.5–1	20–80	2.5–5	1–2	1–5	1–8	2–5	3–15	0.04–0.2
26 May						1.9 ± 0.2	2.5–3	30–45	10–15	5–6	5–15	5–25		5–30	0.1–0.4
24 Oct						6.1 ± 0.8	6.5–7	6–8	30–35	10–15	10–35	10–55		10–60	0.1–0.8
5 Dec						7.4± 0.9	8–8.5	7–9	40–45	15–20	15–45	15–70		20–75	0.3–1.0
2009															
19 Jan						7.6 ± 1.0	8.5–9	1–1.5	40–45	15–20	15–45	15–70		20–75	0.3–1.0
24 Feb						8.5 ± 1.1	9–9.5	5–7	45–50	15–20	15–50	20–75		25–80	0.3–1.1
6 Mar						8.6 ± 1.1	9–9.5	2–4	45–50	15–20	15–50	20–75		25–80	0.3–1.1
18 Apr						9.2 ± 1.2	10–10.5	3–4	50–55	20–25	20–55	20–75		25–80	0.3–1.1
23 Jul						9.6 ± 1.2	10–10.5	1–1.5	50–55	20–25	20–55	25–85		25–90	0.3–1.2
27 Sep						9.2 ± 1.2	10–10.5								
30 Sep						9.7 ± 1.3	10.5–11	0.2–0.4	50–55	20–25	20–55	25–85		25-90	0.3–1.2
2010															
27 Feb						9.8 ± 1.3	10.5–11	0.1–0.2	50–55	20–25	20–55	25–85		25–90	0.3–1.2
26 Nov						10.6 ± 1.4	11–11.5	0.6–0.8	55–60	20–25	25–60	25–90		30–95	0.4–1.3
2011															
28 May						10.0 ± 1.3	11–11.5								
28 Nov						11.0 ± 1.4	12–12.5	0.3–0.4	60–65	20–25	25–65	30–100		30–105	0.4–1.4
2012															
25 Jan						10.9 ± 1.4									
13 Feb						8.7 ± 1.1									
10 Apr						9.9 ± 1.3									

[a]Channel volume estimates assume a 0.5 km^2 deposition over the lower 5 km channel reach.
[b]Volume estimate for delta 1 assumes 1–3 m sediment thickness spread over 0.55 km^2 delta area; it also assumes a lahar deposited 67% of the sediment, and fluvial transport 33%.
[c]Bed load flux rate assumes fluvial fill by 15 May accumulated in 48–72 h. Channel width is assumed to average about 60 m, and volume to mass conversion assumes a sediment deposit bulk density of 1100–1500 kg/m^3. Growth of delta 2 is assumed to have been exclusively bed load delivery.
[d]Assumes a fluvial deposit bulk sediment density of 1100–1500 kg/m^3.
[e]Assumes a bulk deposit density of 1750 kg/m^3.
[f]Normalized to basin area above the bridge in Chaitén town (75 km^2).

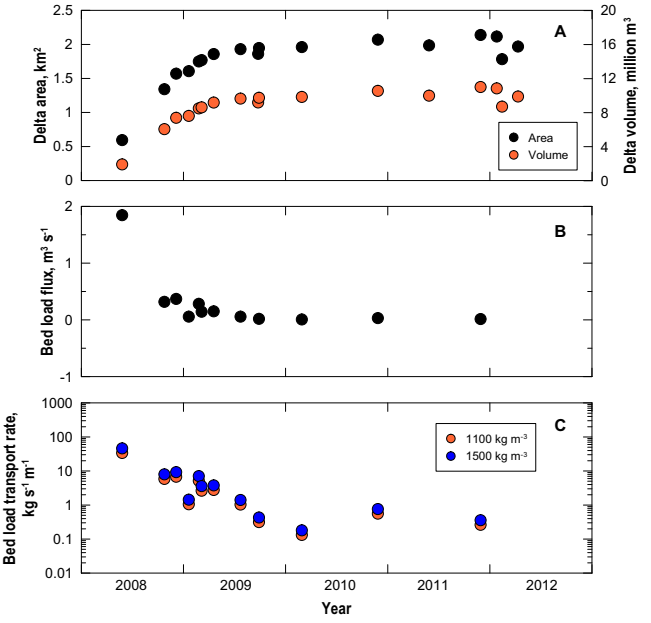

Figure 9. Time series of delta growth and bed load flux at mouth of Chaitén River. (a) Delta area and volume; (b) volumetric bed load flux; (c) bed load mass transport rate.

After the channel avulsed, very high sediment transport continued. A new delta (delta 2), assumed to accumulate sediment transported by traction load, started growing north of the original delta on 14 or 15 May 2008 (Figure 5). By 26 May it had accumulated about $1.9 \pm 0.2 \times 10^6$ m^3 of sediment (Table 3 and Data Set S1 in Supporting Information). The measured mean rate of growth from 14 to 26 May was 1.8 ± 0.2 m^3 s^{-1}, which requires a mean traction-load transport rate of 30–45 kg s^{-1} m^{-1} (Table 3 and Data Set S1 in Supporting Information).

5.1.2. Negro River

First reported observations of Negro River from an overflight on 7 May noted a very turbid, but otherwise unchanged, river [*SERNAGEOMIN*, 2008a]. Subsequently, a major flood event occurred, which we infer coeval with the 11–13 May lahar and flood on Chaitén River. (Low-altitude aerial photographs on 12 May show Negro River in flood.) Flood deposits formed berms on either side of the river channel about 3.2 m above the 2010 river bed, but largely confined within the channel banks. Subsequent surveys from Negro River bridge (Figure 1) show the 2010 bed about 1.8 m above the preeruption bed (Figure S6 in Supporting Information). Topographic position and berm stratigraphy indicate nearly 4 m of continuous aggradation followed by complex erosion and deposition. The lower 2 m of exposed deposit is horizontally bedded, and composed of fresh, gray, pumice-rich, medium to coarse sand with interbeds and lenses of coarse pumice sand and fine gravel (Figure 8C). The horizontally bedded sand grades upward into 0.2 m of ripple-drift cross-bedded similar sand (Figure 8C). Erosional contacts separate this sequence from 0.5 m of darker gray, dune- and ripple-cross-bedded, pumice-rich medium to coarse sand (Figure 8C). As in Chaitén River valley, stratal texture and bedding characteristics indicate initial deposition by dilute hyperconcentrated flow and highly sediment-charged, shallow upper-regime flow which changed to slower lower-regime flow as discharge waned, resistance increased, and transport decreased [*Simons et al.*, 1965; *Collinson and Thompson*, 1989]. There is no evidence of debris-flow lahar.

A substantial length of the Negro River channel accumulated sediment during the flood, but little is known about deposit thickness except locally. Thus, we cannot estimate the volume of sediment flushed from the basin. We can, however, make a rough estimate of traction-load transport rate in an approximately 1 km long reach centered on Negro River bridge near where we examined deposits. In that reach, the channel is 30–50 m wide, deposit thickness relatively uniform, and clearly fluvially deposited sediment 0.75 m thick. These dimensions indicate 20,000–40,000 m^3 of fluvial sediment accumulated here. If we again assume 70% of fluvial sediment accumulated by traction-load transport, then traction load deposited 15,000–30,000 m^3 in the reach. If we also assume this fluvial sediment deposited over the same 2–3 days as that in Chaitén River basin, and that it has a similar bulk density, then we estimate a mean traction-load transport rate of 1.5–8.5 kg s^{-1} m^{-1} per km of channel. This streamwise-normalized mean transport rate, similar to that estimated for lower Chaitén River, shows initial sediment delivery from Negro River basin was also very high.

5.2. Longer-Term Sediment Delivery 2008–2011

Subsequent to the great flush of sediment in the days and weeks after explosive activity waned, sediment supply declined sharply. Delta 2 continued to grow, but at a logarithmically decreasing rate until late 2011 when it reached about 11×10^6 m^3 (Figure 9 and Table 3). By October 2008, delta growth rate had declined to about 0.3 m^3 s^{-1}, and by January 2009 had declined to about 0.06 m^3 s^{-1}. Erosion of the valley-filling

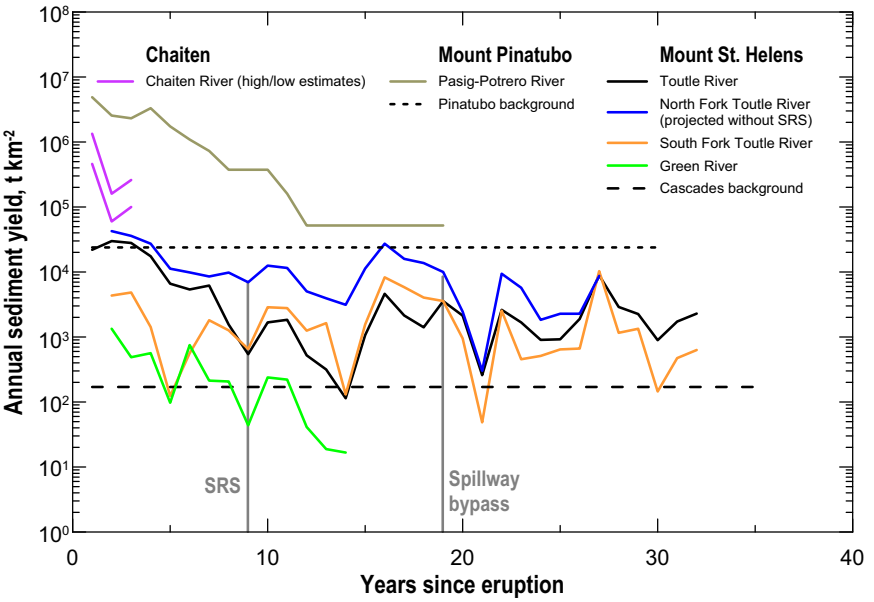

Figure 10. Comparison of mass yields from volcanically disturbed basins at Chaitén, Mount St. Helens, and Mount Pinatubo as functions of time since eruption. The point in time labeled SRS represents the time when a large sediment retention structure began trapping sediment in the Toutle River basin at Mount St. Helens; the point in time labeled spillway bypass represents the time when SRS trap efficiency was greatly reduced and sediment began passing over its spillway. Mount St. Helens yields are based on suspended-sediment load only; those of Mount Pinatubo, like Chaitén, are based mainly on measurements of accumulated deposits. Mount Pinatubo data from *Gran et al.* [2011]; Mount St. Helens data from *Major et al.* [2000] and *Pierson and Major* [2014]. Modified from *Pierson and Major* [2014].

PDC deposit resulting from dome collapse in February 2009 caused delta growth rate to spike by twofold to fivefold for a few months; by July 2009 that sediment-delivery spike had abated (Figure 9 and Table 3). From July 2009 until late 2011, the delta grew at a low and relatively constant rate that averaged about 0.03 $m^3\ s^{-1}$. By about May 2011, delta area and volume stabilized. Persistent negative growth in 2012 indicates wave erosion outpaced sediment influx (Figure 9 and Table 3). Correlative mean traction-load transport rates from October 2008 to December 2011 declined from about 7–0.4 kg $s^{-1}\ m^{-1}$ (Table 3).

On the basis of channel filling and delta growth, Chaitén River transported at least 10×10^6 m^3 of traction load out of the basin in the year following the eruption. At least $2–3 \times 10^6$ m^3, 20–30%, of that traction load was delivered within a couple of weeks in mid to late May 2008. If we assume traction load averaged 20% of total fluvial sediment load, Chaitén River possibly discharged $50–60 \times 10^6$ m^3 of sediment in the first year after eruption, including early mass flow. If we further assume appropriate deposit bulk densities, then total sediment yield for the first year after eruption (including lahar) was about 300–1100 kt km^{-2} (Table 3). For comparison, peak annual sediment yields from basins heavily disturbed by tephra fall and thin ($\leq$1 m) PDC deposits by the 1980 eruption of Mount St. Helens, USA (Green River, Clearwater Creek), and the 2000 eruption of Miyakejima volcano (Japan) were about 1 kt km^{-2} and 1000–2000 kt km^{-2}, respectively [*Major et al.*, 2000; *Tagata et al.*, 2006]. Peak annual yields from basins deeply buried by tens to hundreds of meters of landslide and PDC deposits following the 1980 eruption of Mount St. Helens and 1991 eruption of Mount Pinatubo were about 55 and 2000–8000 kt km^{-2}, respectively (Figure 10) [*Major et al.*, 2000; *Janda et al.*, 1996; *Gran et al.*, 2011]. The Mount Pinatubo eruption—one of the greatest eruptions of the twentieth century—smothered several basins with 5.5 km^3 of PDC deposits and 2 km^3 of tephra-fall deposits [*Paladio-Melosantos et al.*, 1996; *Scott et al.*, 1996]. By contrast, a mere 0.025–0.03 km^3 of tephra-fall and PDC deposits draped Chaitén River basin.

6. Discussion

The hydrogeomorphic responses to landscape disturbance caused by the explosive eruption of Chaitén volcano were not only extremely rapid relative to the onset of a modest rainfall [*Pierson et al.*, 2013], but initial rates of sediment delivery were very high and coeval among proximal basins. In a global context, Chaitén

River basin released one of the greatest modern sediment yields estimated following volcanic disturbance. In the context of Chilean rivers, sediment delivery following the Chaitén eruption vastly exceeded typical sediment transport. Though data are very limited both in numbers of rivers monitored and lengths of sediment records, average annual suspended-sediment yields for some Chilean rivers are on the order of 1–100 t km^{-2} (Data Set S2 in Supporting Information). By contrast, Chaitén River delivered possibly 100–800 kt km^{-2} of suspended sediment during the first year after eruption (Table 3).

6.1. Theoretical Limit of Traction-Load Transport Rate

Estimates of traction-load transport rates at Chaitén, especially in the days and weeks following explosive activity, are very high compared to many other environmental settings. This raises the question of whether they are plausible. For systems having unconstrained sediment supply or availability, *Gomez* [2006] concluded there is an upper, particle-size-dependent limit to bed load transport efficiency. For systems having a dominant bed-material size ranging from 0.002 to 0.2 m (gravel bed rivers), and assuming the rate of bed load transport relates to the rate of energy expenditure [*Bagnold* 1966, 1973], Gomez presents a generalized expression that relates bed load transport rate, stream power, and particle size as

$$i_b = \omega \left[0.0115 \cdot D_{50}^{-0.51}\right]/0.63, \quad (1)$$

where i_b is the transport rate of bed load measured as immersed mass per unit width (kg s^{-1} m^{-1}), ω is stream power per unit channel width (kg s^{-1} m^{-1}), and D_{50} is the bed load median particle size. If we extend this generalized expression to grain sizes beyond the lower bound (0.002 m) posed by *Gomez* [2006], we can roughly estimate potential rate limits of traction-load transport by Chaitén River during the initial sediment flush. Though direct hydraulic measurements are lacking, field evidence indicates flow depth of Chaitén River just prior to avulsion was about 1 m. Samples of the fluvially transported sediment in the upper part of the channel fill have D_{50} ranging from 0.0001 to 0.0006 m [*Pierson et al.*, 2013]. Slope of the lower 3 km of Chaitén River channel, estimated from Google Earth, averages 0.005 m/m. If we assume flow velocity in the shallow, braided river condition indicated by sediment texture ranged from 2 to 4 m s^{-1}, equation (1) indicates potential rates of traction-load transport during the initial sediment flush may have ranged from 8 to 40 kg s^{-1} m^{-1}. These theoretically upper-limit rates of transport are broadly consistent with our estimates of mean transport rates based on rates and magnitudes of channel filling, delta growth, and sedimentological interpretations. Though Gomez' expression is not strictly applicable to conditions at Chaitén, this analysis indicates our estimated mean transport rates, though very high, are plausible. Unlike river systems in many other settings, Chaitén River largely transported low-density pumice and lithic rhyolite sand, especially during the earliest phases of response.

Clearly, our estimated mean transport rates are subject to substantial data limitations. Measurements of channel-fill thickness, the time over which the channel filled, and changes in visible delta area are well constrained. The high fines content within the fluvial part of the channel fill [*Pierson et al.*, 2013], indicative of flow moving much suspended sediment, limits our ability to determine precisely the amount and composition of sediment deposited solely by traction load. We estimate traction load deposited about 70% of the fluvial channel fill (see *Visher*, 1969), but it could be less. The time series of delta volume assumes sediment is uniformly distributed, estimated thickness is plausible, and all sediment accumulated by traction load. Measurements of sediment thickness (15–17 m) in a vastly smaller mountain fan-delta in British Columbia [*Pelpola and Hicken*, 2004] indicate our estimate of about 10 m sediment thickness at Chaitén (Data Set S1 in Supporting Information) is plausible. Our greatest unknowns regard the magnitude of sediment that bypassed the delta and the relation of traction load to total sediment load. Turbid plumes evident in satellite imagery clearly show sediment (largely suspended load) moved beyond the visible limit of the delta. If a large amount of traction load bypassed the visible delta surface and deposited along the steep delta front, temporal estimates of delta volumes, as well as traction-load transport rates, are even greater. At present, we cannot confidently constrain the volume of sediment that may have accumulated on the delta front. On the basis of measurements worldwide, our assumption that traction load may represent 20–50% of total sediment load seems a reasonable bounding range.

6.2. Sediment Source Evolution

The dominant sediment source in Chaitén River basin evolved as erosion proceeded following volcanic disturbance. Peak transport delivered predominantly fresh tephra, which indicates eroded new material, not

remobilized older sediment, was the dominant sediment source at that time. A lack of landslides shows rill and gully erosion the dominant erosional and delivery process from hillsides to the channel. After the initial sediment flush newly deposited channel fill and older channel sediment became important contributing sources. Analysis of tephra-fall isopachs and in situ deposits indicates at least 25 $\times$ 10^6 m^3, and perhaps 30 $\times$ 10^6 m^3, of tephra-fall deposit drapes the basin (Table 2). A pair of pyroclastic density currents subsequently delivered an additional 3–5 $\times$ 10^6 m^3. Thus, the eruption delivered perhaps 30–35 $\times$ 10^6 m^3 of sediment to the basin. By late May 2008, total sediment delivery from the basin possibly ranged from 6 to 18 $\times$ 10^6 m^3 (Table 3). Thus, the initial weeks of erosion removed a large fraction of the tephra fall delivered to the basin. One year after the eruption, Chaitén River possibly discharged 15–55 $\times$ 10^6 m^3 of sediment. These discharge estimates, along with observations in 2010 of substantial remnants of in situ tephra-fall and PDC deposits [*Major and Lara*, 2013; *Major et al*., 2013; *Pierson et al*., 2013] as well as substantial channel incision, indicate eroded channel fill from the 2008–2009 and older eruptions had become an important contributing sediment source. By December 2011, perhaps 25–70 $\times$ 10^6 m^3 of sediment had been discharged (Table 3). These estimated values of sediment delivery, combined with field observations, indicate eroded channel sediment became the dominant sediment source, perhaps no more than a year after the eruption. Eroded channel sediment consisted of fill deposited by the initial sediment flush, by subsequent PDCs, and remanent sediment from older eruptions.

Analyses of changes in channel width and channel pattern of Chaitén River support the inferences drawn above. *Ulloa et al*. [2015a, 2016] documented significant increases in active channel width, changes from a single-thread to a multithread channel pattern, and changes in channel sinuosity and other planform morphologies between a preeruption image and a posteruption image from late 2009. These morphological changes show channel banks were actively eroded no later than a year or so after the eruption. A later image from January 2012 shows persistent bank erosion [*Ulloa et al*., 2015a].

6.3. Causes of Erosional and Transport Efficiency

Multiple factors contributed to the efficient erosion and transport of sediment at Chaitén. We attribute the magnitude of erosion and extremely efficient transport of fresh tephra-fall deposit at Chaitén to (a) sufficiently thick and fine-grained upper tephra layers that drastically reduced infiltration capacity on basin slopes, (b) the high relief and steepness of drainage basin slopes [*Pierson et al*., 2013], and (c) the low density of the particles transported. At Usu volcano (Japan) and Mount St. Helens, only about 10–20% of tephra-fall deposits were eroded within 1–4 years of eruption because erosion shut down once rills and gullies incised through relatively thin layers of fine ash and exposed coarser ash [*Kadomura et al*., 1983; *Collins and Dunne*, 1986]. At Chaitén, the thick (tens of cm) mantle of fine to extremely fine ash (silty sand) (Figure 4) in basin headwaters allowed a prolonged period of overland flow after incision of the tephra layer began, which led to more widespread and efficient tephra erosion. Much of the substantial erosion of tephra-fall deposits at Chaitén occurred within weeks whereas erosion of comparable fractions of tephra deposits took months to years at other volcanoes. Overall steepness of the basin provides for potentially large stream power, and the low particle density of the volcanic sediment likely enhanced transport capability.

6.4. Rates of Channel Adjustments Toward Preeruption Conditions

Chaitén River channel reestablished nearly preeruption bed level (Figures S6 and S7 in Supporting Information), channel pattern and dimensions [*Ulloa et al*., 2015a, 2016], and bed material size (Data Set S3 in Supporting Information) by March 2012, slightly less than 4 years after massive volcanic sediment loading. This rate of apparent recovery is remarkably fast compared to some other rivers affected by severe volcanic disturbances (Table S1 in Supporting Information). Minor fluctuations in bed elevations and textures and adjustments to cross-section areas occurred from January 2013 to 2015 (Figure S6 in Supporting Information). These secondary fluctuations in channel geometry and bed texture in active volcanic rivers are ordinary [e.g., *Gran*, 2012; *Zheng et al*., 2014; *Mosbrucker et al*., 2015], and are common following primary adjustments to great sediment inputs [e.g., *Podolak and Wilcock*, 2013]. Local rates of geomorphic recovery of Chaitén River channel are similar to those of basins at Mount St. Helens and Mount Pinatubo affected by only tephra-fall deposits or draped thinly by deposits from PDCs [*Meyer and Martinson*, 1989; *Gran and Montgomery*, 2005] (Table S1 in Supporting Information).

The geomorphic response following eruption of Chaitén volcano provides further evidence that, in general, the magnitude and duration of response to volcanic disturbance relates strongly to the nature of

disturbance and geomorphic regime that is disturbed [e.g., *Major et al*., 2000; *Gran and Montgomery*, 2005; *Gran et al*., 2011; *Pierson and Major*, 2014]. The greatest magnitude and longest duration (decades or more) channel changes, as well as persistently elevated sediment yields, have occurred after eruptions that have caused exceptional disturbance to river channels (widespread deposition of channel fills tens of meters thick and in excess of 10×10^6 m^3). By contrast, geomorphic responses to hillside disturbances and to more moderate channel disturbances, though potentially intense and capable of causing significant socioeconomic harm, are relatively short-lived—years, not decades—unless hillsides and channels are persistently recharged with tephra falls and other volcaniclastic sediment from frequent eruptive activity (e.g., Santiaguito dome complex [*Harris et al*., 2006] and Sakurajima volcano [*Iguchi et al*., 2013]). These patterns of response duration—borne out over several eruptions at other volcanoes over the past few decades, and also noted following dam removals [e.g., *East et al*., 2015; *Magirl et al*., 2015]—may provide emergency management and other governmental officials some insights on the length of time they may need to cope with challenging fluvial responses to volcanic eruptions.

7. Conclusions

Results of this study show unusual sediment delivery by rivers draining terrain on or near Chaitén volcano was both very high and short-lived following its 2008–2009 eruption. Following onset of modest, low-intensity rainfall during the waning phase of explosive activity in mid May 2008, an extraordinary and coeval flush of sand and silt-rich sediment discharged from multiple basins around the volcano. Substantial alteration of the hillslope hydrological regime by significant vegetation damage and thick accumulation (as much as 200 cm) of fine-grained tephra-fall in basin headwaters triggered extensive rill and gully erosion—there were few if any landslides. Exceptional aggradation of Chaitén River channel within a matter of days caused the river to avulse through a coastal town 10 km downstream from the volcano. On the basis of rates and magnitudes of channel aggradation and delta growth in Chaitén Bay, we conclude the initial sediment flush involved very high traction-load transport rates, possibly as great as several tens of kg s^{-1} m^{-1}, for many weeks. Subsequent delta growth shows traction-load transport rates declined sharply. From October 2008 to December 2011, mean transport rates declined logarithmically from about 7 to 0.4 kg s^{-1} m^{-1}. In a global context, Chaitén River basin released one of the greatest modern annual sediment yields estimated following volcanic disturbance. Within a year of eruption, Chaitén River likely delivered $25–80 \times 10^6$ t, equivalent to $0.3–1 \times 10^6$ t km^{-2}.

Despite very high rates and magnitudes of sediment delivery, rates of channel recovery were rapid. At locations near bridges in medial to distal reaches of Chaitén and Negro River channels, which had aggraded by 4–7 m within days of the onset of sediment release, preeruption channel bed elevations were regained within 3–7 years, channel planforms reverted to preeruption planforms within a couple of years [*Ulloa et al*., 2015a, 2016], and bed-sediment textures coarsened significantly within 3–4 years. These locally observed rates of channel recovery, if representative, show impacted channels achieved at least states of quasi-stability swiftly after the eruption. Recovery rates at Chaitén are similar to those in volcanically disturbed basins elsewhere having hillsides draped in tephra fall but having channels that were relatively little affected by primary volcaniclastic input. Rates of recovery at Chaitén provide further evidence that geomorphic responses to hillside disturbances or moderate channel disturbances, though potentially intense and capable of causing significant socioeconomic harm, are relatively short-lived—years, not decades—unless hillsides and channels are persistently recharged with tephra falls and volcaniclastic sediment from frequent eruptions.

Acknowledgments
We thank Ben Mirus and Christian Mohr for encouraging this contribution. The U.S. Geological Survey Volcano Science Center, SERNAGEOMIN's Programa de Riesgos Volcánicos, Conicyt Fondecyt grants 1110609, 1141064, and 11130671, Conicyt Fondap grant 15090013, and the Vamos Research Centre provided support. Fred Swanson, Charlie Crisafulli, and Rick Hoblitt provided field assistance and graciously shared data. Data supporting transport computations, comparisons, and interpretations are provided in Supporting Information. We thank John Laronne, Basil Gomez, James Bathurst, and an anonymous reviewer for their insightful comments and critiques of an earlier version of this paper. Any use of trade, firm, or product names is for descriptive purposes only and does not imply endorsement by the U.S. Government.

References

Alfano, F., C. Bonadonna, A. C. M. Volentik, C. B. Connor, S. F. L. Watt, D. M. Pyle, and L. J. Connor (2011), Tephra stratigraphy and eruptive volume of the May, 2008, Chaitén eruption, Chile, *Bull. Volcanol.*, *73*, 613–630.

Alfano, F., C. Bonadonna, and L. Gurioli (2012), Insights into eruption dynamics from textural analysis: The case of the May, 2008, Chaitén eruption, *Bull. Volcanol.*, *74*, 2095–2108.

Ayris, P. M., and P. Delmelle (2012), The immediate environmental effects of tephra emission, *Bull. Volcanol.*, *74*, 1905–1936.

Bagnold, R. A. (1966), An approach to the sediment transport problem from general physics, *U.S. Geol. Surv. Prof. Pap.*, *422*-I, pp. I1–I37.

Bagnold, R. A. (1973), The nature of saltation and of "bed-load" transport in water, *Proc. R. Soc. Lond., Series A*, *322*, 473–504.

Bagnold, R. A. (1977), Bed load transport by natural rivers, *Water Resour. Res.*, *13*, 303–312.

Barclay, J., J. Alexander, and J. Sŭsnik (2007), Rainfall-induced lahars in the Belham Valley, Montserrat, West Indies, *J. Geol. Soc. London*, *164*, 815–817.

Bonadonna, C., and A. Costa (2013), Modeling tephra sedimentation from volcanic plumes, in *Modeling Volcanic Processes: The Physics and Mathematics of Volcanism*, edited by S. A. Fagents, T. K. P. Gregg, and R. M. C. Lopes, pp. 173–202, Cambridge Univ. Press, Cambridge, U. K.
Carn, S. A., J. S. Pallister, L. Lara, J. W. Ewert, S. Watt, A. J. Prata, R. J. Thomas, and G. Villarosa (2009), The unexpected awakening of Chaitén volcano, Chile, *Eos Trans AGU*, *90*, 205–212.
Castro, J. M., and D. B. Dingwell (2009), Rapid ascent of rhyolitic magma at Chaitén volcano, Chile, *Nature*, *461*, 780–784.
Childers, D. (1999), Field comparisons of six pressure-difference bedload samplers in high-energy flow, *U.S. Geol. Surv. Water Resour. Invest. Rep.*, *92*–4068, 59 pp.
Cohen, H., and J. B. Laronne (2005), High rates of sediment transport by flashfloods in the Southern Judean Desert, Israel, *Hydrol. Proc.*, *19*, 1687–1702.
Collins, B. D., and T. Dunne (1986), Erosion of tephra from the 1980 eruption of Mount St. Helens, *Geol. Soc. Am. Bull.*, *97*, 896–905.
Collinson, J. D., and D. B. Thompson (1989), *Sedimentary Structures*, 2nd ed., 207 pp., Unwin Hyman, London, U. K.
Crisafulli, C. M., F. J. Swanson, J. J. Halvorson, and B. D. Clarkson (2015), Volcano ecology: Disturbance characteristics and assembly of biological communities, in *The Encyclopedia of Volcanoes*, 2nd ed., edited by H. Sigurdsson et al., pp. 1265–1284, Academic, San Diego, Calif.
Dietrich, W. E., and J. D. Smith (1984), Bedload transport in a river meander, *Water Resour. Res.*, *20*, 1355–1380.
Dirección General de Aguas (2015), *Estadística Hidrológica en Linea*. [Available at www.dga.cl.]
East, A. E., et al. (2015), Large-scale dam removal on the Elwha River, Washington, USA: River channel and floodplain geomorphic change, *Geomorphology*, *228*, 765–786.
Fundación Huinay (2015), *Climate pluviometry*, Puerto Montt. [Available at http://fundacionhuinay.cl/climate.html.]
Gaeuman, D., and R. B. Jacobson (2006), Acoustic bed velocity and bed load dynamics in a large sand bed river, *J. Geophys. Res.*, *111*, F02005, doi:10.1029/2005JF000411.
Garreaud, R. D. (2009), The Andes climate and weather, *Adv. Geosci.*, *22*, 3–11.
Gaweesh, M. T. K., and L. C. van Rijn (1994), Bed-load sampling in sand-bed rivers, *J. Hydraul. Eng.*, *120*, 1364–1384.
Gomez, B. (2006), The potential rate of bed-load transport, *Proc. Nat. Acad. Sci.*, *103*, 17170–17173.
Gran, K. B. (2012), Strong seasonality in sand loading and resulting feedbacks on sediment transport, bed texture, and channel planform at Mount Pinatubo, Philippines, *Earth Surf. Proc. Landforms*, *37*, 1012–1022.
Gran, K. B., and D. R. Montgomery (2005), Spatial and temporal patterns in fluvial recovery following volcanic eruptions–channel response to basin-wide sediment loading at Mount Pinatubo, Philippines, *Geol. Soc. Am. Bull.*, *117*, 195–211.
Gran, K. B., D. R. Montgomery, and J. C. Halbur (2011), Long-term elevated post-eruption sedimentation at Mount Pinatubo, Philippines, *Geology*, *39*, 367–370.
Hammond, S. E. (1989), Comparison of sediment transport formulas and computation of sediment discharges for the North Fork Toutle and Toutle Rivers, near Mount St. Helens, Washington, U.S. *Geol. Surv. Open File Rep.*, *88*-463, 18 pp.
Harris, A. J. L., J. W. Vallance, P. Kimberly, W. I. Rose, O. Matías, E. Bunzendahl, L. P. Flynn, and H. Garbeil (2006), Downstream aggradation owing to lava dome extrusion and rainfall runoff at Volcán Santiaguito, Guatemala, in *Volcanic Hazards in Central America*, edited by W. I. Rose et al., Geol. Soc. Am. Bull. Spec. Pap., 412, 85–104.
Hayes, S. K., D. R. Montgomery, and C. G. Newhall (2002), Fluvial sediment transport and deposition following the 1991 eruption of Mount Pinatubo, *Geomorphology*, *45*, 211–224.
Iguchi, M., T. Tameguri, Y. Ohta, S. Ueki, and S. Nakao (2013), Characteristics of volcanic activity at Sakurajima Volcano's Showa crater during the period 2006 to 2011, *Bull. Volcanol. Soc. Jpn.*, *58*, 115–135.
Janda, R. J., D. F. Meyer, and D. Childers (1984), Sedimentation and geomorphic changes during and following the 1980–1983 eruptions of Mount St. Helens, Washington, *Shin Sabo*, *37*(2), 10–21, and 37(3), 5–19.
Janda, R. J., A. S. Daag, P. J. Delos Reyes, C. G. Newhall, T. C. Pierson, R. S. Punongbayan, K. S. Rodolfo, R. U. Solidum, and J. V. Umbal (1996), Assessment and response to lahar hazard around Mount Pinatubo, 1991 to 1993, in *Fire and Mud: Eruptions and Lahars of Mount Pinatubo, Philippines*, edited by C. G. Newhall and R. S. Punongbayan, pp. 107–193, Univ. of Wash. Press, Seattle.
Jones, R., V. Manville, and D. Andrade (2015), Probabilistic analysis of rainfall-triggered lahar initiation at Tungurahua volcano, *Bull. Volcanol.*, *77*(8), 68.
Kadomura, H., T. Imagawa, and H. Yamamoto (1983), Eruption-induced rapid erosion and mass movements on Usu Volcano, Hokkaido, *Z. Geomorph. NF Suppl. Band*, *46*, 123–142.
Lara, L. E. (2009), The 2008 eruption of the Chaitén Volcano, Chile: A preliminary report, *Andean Geol.*, *36*, 125–129.
Lara, L. E., R. Moreno, Á. Amigo, R. P. Hoblitt, and T. C. Pierson (2013), Late Holocene history of Chaitén Volcano—New evidence for a 17th-century eruption, *Andean Geol.*, *40*(2), 249–261.
Laronne, J. B., and I. Reid (1993), Very high rates of bed load sediment transport by ephemeral desert rivers, *Nature*, *336*, 148–150.
Lavigne, F., J. C. Thouret, B. Voight, H. Suwa, and A. Sumaryono (2000), Lahars at Merapi volcano, Central Java: An overview, *J. Volcanol. Geotherm. Res.*, *100*, 423–456.
Leavesley, G. H., G. C. Lusby, and R. W. Lichty (1989), Infiltration and erosion characteristics of selected tephra deposits from the 1980 eruption of Mount St. Helens, Washington, USA, *Hydrol. Sci. J.*, *34*, 339–353.
Magirl, C. S., R. C. Hilldale, C. A. Curran, J. J. Duda, T. D. Straub, M. Domanski, and J. R. Foremann (2015), Large-scale dam removal on the Elwha River, Washington, USA: Fluvial sediment load, *Geomorphology*, *246*, 669–686.
Major, J. J., and L. E. Lara (2013), Overview of Chaitén Volcano, Chile, and its 2008–2009 eruption, *Andean Geol.*, *40*(2), 196–215.
Major, J. J., and L. E. Mark (2006), Peak flow responses to landscape disturbances caused by the cataclysmic 1980 eruption of Mount. St. Helens, Washington, *Geol. Soc. Am. Bull.*, *118*, 938–958.
Major, J. J., T. C. Pierson, R. L. Dinehart, and J. E. Costa (2000), Sediment yield following severe volcanic disturbance—A two-decade perspective from Mount St. Helens, *Geology*, *28*, 819–822.
Major, J. J., et al. (2012), Geomorphic response of the Sandy River, Oregon, to removal of Marmot Dam, *U.S. Geol. Surv. Prof. Pap.*, *1792*, 64 pp.
Major, J. J., T. C. Pierson, R. P. Hoblitt, and H. Moreno (2013), Pyroclastic density currents associated with the 2008–2009 eruption of Chaitén Volcano (Chile): Forest disturbances, deposits, and dynamics, *Andean Geol.*, *40*(2), 324–358.
Meyer, D. F., and H. A. Martinson (1989), Rates and processes of channel development and recovery following the 1980 eruption of Mount St. Helens, Washington, *Hydrol. Sci. J.*, *34*, 115–127.
Miyabuchi, Y. (1999), Deposits associated with the 1990–1995 eruption of Unzen volcano, Japan, *J. Volcanol. Geotherm. Res.*, *89*, 139–158.
Montgomery, D. R., M. S. Panfil, and S. K. Hayes (1999), Channel-bed mobility response to extreme sediment loading at Mount Pinatubo, *Geology*, *27*, 271–274.
Moreno, P. I., B. V. Alloway, G. Villarosa, V. Outes, W. I. Henriquez, R. De Pol-Holz, and N. J. G. Pearce (2015), A past-millenium maximum in postglacial activity from Volcán Chaitén, southern Chile, *Geology*, *43*, 47–50.

Mosbrucker, A. R., K. R. Spicer, J. J. Major, D. R. Saunders, T. S. Christianson, and C. G. Kingsbury (2015), Digital database of channel cross-section surveys, Mount St. Helens, Washington, *U.S. Geol. Surv. Data Ser.*, *951*, 9 pp.

Newhall, C. G., and S. Self (1982), The volcanic explosivity index (VEI): An estimate of explosive magnitude for historical eruptions, *J. Geophys. Res.*, *87*(C2), 1231–1238.

Ogawa, Y., H. Daimaru, and A. Shimizu (2007), Experimental study of post-eruption overland flow and sediment load from slopes overlain by pyroclastic-flow deposits, Unzen volcano, Japan, *Géomorphol. Relief Proc. Environ.*, *3*, 237–246.

Paladio-Melosantos, M. L. O., R. U. Solidum, W. E. Scott, R. B. Quiambao, J. V. Umbal, K. S. Rodolfo, B. S. Tubianosa, P. J. Delos Reyes, R. A. Alonso, and H. B. Ruelo (1996), Tephra falls of the 1991 eruptions of Mount Pinatubo, in *Fire and Mud: Eruptions and Lahars of Mount Pinatubo, Philippines*, edited by C. G. Newhall and R. S. Punongbayan, pp. 513–535, Univ. of Wash. Press, Seattle.

Pallister, J. S., A. K. Diefenbach, W. C. Burton, J. Muñoz, J. P. Griswold, L. E. Lara, J. B. Lowenstern, and C. E. Valenzuela (2013), The Chaitén rhyolite lava dome: Eruption sequence, lave dome volumes, rapid effusion rates and source of the rhyolite magma, *Andean Geol.*, *40*(2), 277–294.

Pelpola, C. P., and E. J. Hickin (2004), Long-term bed load transport rate based on aerial-photo and ground penetrating radar surveys of fan-delta growth, Coast Mountains, British Columbia, *Geomorphology*, *57*, 169–181.

Pierson, T. C. (2005), Hyperconcentrated flow—Transitional process between water flow and debris flow, in *Debris-Flow Hazards and Related Phenomena*, edited by M. Jakob and O. Hungr, pp. 159–202, Springer-Praxis, Berlin.

Pierson, T. C., and J. J. Major (2014), Hydrogeomorphic effects of explosive volcanic eruptions on drainage basins, *Ann. Rev. Earth Planet. Sci.*, *42*, 469–507.

Pierson, T. C., J. J. Major, Á. Amigo, and H. Moreno (2013), Acute sedimentation response to rainfall following the explosive phase of the 2008–2009 eruption of Chaitén volcano, Chile, *Bull. Volcanol.*, *75*(5), 723.

Pitlick, J. (1992), Flow resistance under conditions of intense gravel transport, *Water Resour. Res.*, *28*, 891–903.

Pitlick, J., Y. Cui, and P. Wilcock (2009), Manual for computing bed load transport using BAGS (Bedload Assessment for Gravel-bed Streams) software, *Gen. Tech. Rep. RMRS-GT-223*, 45 pp., U.S. Dept. Agric., For. Serv., Rocky Mt. Res. Stn., Fort Collins, Colo.

Podolak, C. J. P., and P. R. Wilcock (2013), Experimental study of the response of a gravel streambed to increased sediment supply, *Earth Surf. Proc. Landforms*, *38*, 1748–1764.

Prata, A. T., S. T. Siems, and M. J. Manton (2015), Quantification of volcanic cloud top heights and thicknesses using A-train observations for the 2008 Chaitén eruption, *J. Geophy. Res. Atmos.*, *120*, 2928–2950, doi:10.1002/2014JD022399.

Pratt-Sitaula, B., M. Garde, D. W. Burbank, M. Oskin, A. Heimsath, and E. Gabet (2007), Bedload-to-suspended load ratio and rapid rock incision from Himalayan landslide-dam record, *Quat. Res.*, *68*, 111–120.

Punongbayan, R. S., C. G. Newhall, and R. P. Hoblitt (1996), Photographic record of rapid geomorphic change at Mount Pinatubo, 1991–94, in *Fire and Mud: Eruptions and Lahars of Mount Pinatubo, Philippines*, edited by C. G. Newhall and R. S. Punongbayan, pp. 21–66, Univ. of Wash. Press, Seattle.

Reid, I., J. C. Bathurst, P. A. Carling, D. E. Walling, and B. W. Webb (1997), Sediment erosion, transport, and deposition, in *Applied Fluvial Geomorphology for River Engineering and Management*, edited by C. R. Thorne, R. D. Hey, and M. D. Newson, pp. 95–135, John Wiley, Chichester, U. K.

Rennie, C. D., and P. V. Villard (2004), Site specificity of bed load measurement using an acoustic Doppler current profiler, *J. Geophys. Res.*, *109*, F03003, doi:10.1029/2003JF000106.

Scott, W. E., R. P. Hoblitt, R. C. Torres, S. Self, M. N. L. Martinez, and T. Nillos (1996), Pyroclastic flows of the June 15, 1991, climactic eruption of Mount Pinatubo, in *Fire and Mud: Eruptions and Lahars of Mount Pinatubo, Philippines*, edited by C. G. Newhall and R. S. Punongbayan, pp. 545–570, Univ. of Wash. Press, Seattle.

SERNAGEOMIN (2008a), Erupción del Volcan Chaitén, Informe Técnico 3, 07 de Mayo de 2008. OVDAS-SERNAGEOMIN, Servicio Nacional de Geología y Minería, Santiago.

SERNAGEOMIN (2008b), Erupción del Volcan Chaitén, Informe Técnico 10, 15 de Mayo de 2008. OVDAS-SERNAGEOMIN, Servicio Nacional de Geología y Minería, Santiago.

Servicio Hidrográfico y Oceanográfico de la Armada de Chile (1999), Ensenada Chaitén, 1:20,000, Valparaiso.

Simons, D. B., E. V. Richardson, and C. F. Nordin Jr. (1965), Sedimentary structures generated by flow in alluvial channels, *Soc. Econ. Paleontol. Mineral.*, *12*, 34–52.

Swanson, F. J., J. A. Jones, C. M. Crisafulli, and A. Lara (2013), Effects of volcanic and hydrologic processes on forest vegetation, Chaitén Volcano, Chile, *Andean Geol.*, *40*(2), 359–391.

Tagata, S., T. Yamakoshi, Y. Doi, J. Kurihara, H. Terada, and N. Sakai (2006), Posteruption characteristics of rainfall runoff and sediment discharge at the Miyakejima Volcano, Japan, in *Proceedings of the INTERPRAEVENT International Symposium*, pp. 291–301, Univ. Academic Press, Tokyo.

Turowski, J. M., D. Rickenmann, and S. J. Dadson (2010), The partitioning of the total sediment load of a river into suspended load and bedload: A review of empirical data, *Sedimentology*, *57*, 1126–1146.

Ulloa, H., A. Iroumé, L. Mao, A. Andreoli, S. Diez, and L. E. Lara (2015a), Use of remote imagery to analyse changes in morphology and longitudinal large wood distribution in the Blanco River after the 2008 Chaitén volcanic eruption, southern Chile, *Geogr. Ann., Ser. A*, *97*, 523–541.

Ulloa, H., A. Iroumé, L. Picco, O. Korup, M. A. Lenzi, L. Mao, and D. Ravazzolo (2015b), Massive biomass flushing despite modest channel response in the Rayas River following the 2008 eruption of Chaitén volcano, Chile, *Geomorphology*, *250*, 397–406.

Ulloa, H., A. Iroumé, L. Picco, C. H. Mohr, B. Mazzorana, M. A. Lenzi, and L. Mao (2016), Spatial analysis of the impacts of the Chaitén volcano eruption (Chile) in three fluvial systems, *J. South Am. Earth Sci.*, *69*, 213–225.

Umazano, A. M., R. N. Melchor, E. Bedatou, E. S. Bellosi, and J. M. Krause (2014), Fluvial response to sudden input of pyroclastic sediment during the 2008–2009 eruption of the Chaitén Volcano (Chile): The role of logjams, *J. South Am. Earth Sci.*, *54*, 140–157.

Umbal, J. V. (1997), Five years of lahars at Pinatubo Volcano: Declining but still potentially lethal hazards, *J. Geol. Soc. Philipp.*, *52*, 1–19.

Visher, G. S. (1969), Grain size distributions and depositional processes, *J. Sed. Petrol.*, *39*, 1074–1106.

Waldron, H. H. (1967), Debris flow and erosion control problems caused by the ash eruptions of Irazú volcano, Costa Rica, *U.S. Geol. Surv. Bull.*, *1241* I, 37 pp.

Wallick, J. R., S. W. Anderson, C. Cannon, and J. E. O'Connor (2010), Channel change in the lower Chetco River, Oregon, *U.S. Geol. Surv. Sci. Invest. Rep.*, *5065*, 68 pp.

Watt, S. F. L., D. M. Pyle, T. A. Mather, R. S. Martin, and N. E. Matthews (2009), Fallout and distribution of volcanic ash over Argentina following the May 2008 explosive eruption of Chaitén, Chile, *J. Geophys. Res.*, *114*, B04207, doi:10.1029/2008JB006219.

Watt, S. F. L., D. M. Pyle, and T. A. Mather (2013), Evidence of mid- to late-Holocene explosive rhyolitic eruptions from Chaitén Volcano, Chile, *Andean Geol.*, *40*(2), 216–226.

White, J. D. L., and B. F. Houghton (2006), Primary volcaniclastic rocks, *Geology*, *34*, 677–680.
White, J. D. L., B. F. Houghton, K. A. Hodgson, and C. J. N. Wilson (1997), Delayed sedimentary response to the A.D. 1886 eruption of Tarawera, New Zealand, *Geology*, *25*, 459–462.
Wilcox, A. C., J. E. O'Connor, and J. J. Major (2014), Rapid reservoir erosion, hyperconcentrated flow, and downstream deposition triggered by breaching of 38 m tall Condit Dam, White Salmon River, Washington, *J. Geophys. Res. Earth Surf*, *119*, 1376–1394, doi:10.1002/2013JF003073.
Wohl, E. (2000), Mountain Rivers, *AGU Water Resour. Monogr.*, *14*, 320 pp.
Yamakoshi, T., Y. Doi, and N. Osanai (2005), Post-eruption hydrology and sediment discharge at the Miyakejima volcano, Japan, *Z. Geomorph. NF Suppl. Band*, *140*, 55–72.
Zheng, S., B. Wu, C. R. Thorne, and A. Simon (2014), Morphological evolution of the North Fork Toutle River following the eruption of Mount St. Helens, Washington, *Geomorphology*, *208*, 102–116.